IMPORTANCE OF CRACK TUNNELING DURING FRACTURE: EXPERIMENTS AND CTOA ANALYSES

M. A. James[1] and J. C. Newman, Jr.[2]

[1]National Research Council Associate and [2]Senior Scientist
NASA Langley Research Center, Hampton, Virginia, 23681, USA

ABSTRACT

This paper compares experimental crack-front shapes recorded at various stages of crack extension with area-average crack-extension values during fracture tests conducted on 2024-T351 aluminum alloy plate. Crack-front shapes were determined by fracturing the specimen to a predetermined amount of crack extension, and fatigue cycling the specimen for about 2,000 cycles at a high stress ratio (P_{min}/P_{max}) to mark the crack-front location. For each shape, the area-average crack length was determined. The evolution of tunneling was used to create a calibration curve that could be used to adjust surface measured crack length values, for a more representative comparison with analyses that use a straight crack-front approximation. The analysis compares much more favorably with the average crack extension than with the surface measured values near maximum load. However, the area average technique tends to over correct crack extension near the crack initiation load. Crack tunneling results show that the area average technique produces more representative crack-length measurements compared to optical based surface measurements.

KEYWORDS

CTOA, crack extension, unloading compliance, area-average, tunneling, finite-element analysis

INTRODUCTION

During the 1990's, as part of a national aging aircraft program, NASA Langley Research Center (LaRC) conducted intensive research on the fracture behavior of thin sheet aluminum alloys [1]. Some of the products of that research were the constant critical crack-tip-opening-angle (CTOA, Ψ_c) fracture criterion, optical/digital imaging means for measuring CTOA, and optical methods for measuring surface crack extension [2]. Two additional means of measuring crack extension, unloading compliance and area average, were not used in favor of the optical methods. This paper presents a comparison of experimental crack-front shapes recorded at various stages of crack extension with area-average crack extension values, and shows how these various measures compare with surface measured values and typical finite-element predictions.

BACKGROUND

Wells [3] originally proposed the use of the crack-tip-opening displacement (CTOD) or angle (CTOA) during his experimental work. CTOA (Ψ_c) is usually applied as the angle formed by stable tearing material measured at a fixed distance, d, behind the moving crack (typically, d is taken as 1 mm). The fracture methodology developed as part of the NASA program assumes that the critical CTOA is constant and independent of loading and in-plane configuration, as long as the crack length is about 4 times the plate thickness. The criterion has been applied in both two-dimensional (2D) and three-dimensional (3D) finite-element analysis (FEA). Inherent in 2D FEA is the approximation that the crack front is flat and straight through the thickness of the model. However, neither plane stress nor plane strain accurately capture both

the local stress triaxiality near the crack tip and the plane-stress behavior remote from the crack. Three-dimensional analyses with a flat, straight crack-front maintain a straightforward modeling approach, yet capture the complex constraint behavior missing from typical 2D analysis. The methodology is applied by finding Ψ_c such that the analysis matches the average maximum load for coupon tests (typically, compact tension, W = 152 mm, specimen). This angle is used in subsequent analyses for predictions of crack extension and fracture.

Figure 1 shows a schematic of a typical fracture surface. Initially, the material fails in tension, most likely due to micro-void coalescence. Tunneling occurs on the interior, and shear bands start on the surface and eventually join to form a single shear dominated fracture surface.

Recently, a wide variety of fracture tests were conducted on 6.35 mm thick 2024-T351 aluminum alloy [4]. Both C(T) (compact tension) and M(T) (middle-crack tension) specimens were tested. Figure 2 shows selected load-crack extension results, including both test and analysis results. The 152 mm wide C(T) was used to find Ψ_c, the critical value of CTOA, by matching the average maximum load for the tests. This value of Ψ_c was used to predict the behavior of the other C(T) and M(T) configurations. The results show that the constant critical CTOA fracture criterion is transferable between C(T) specimens and M(T) specimens and show that the analysis was able to accurately predict the maximum load for C(T) specimens ranging in size from 50 mm to 152 mm and for M(T) specimens ranging in size from 75 mm to 1016 mm.

A consistent observation made of these load-crack extension curves (and similar curves for other thin sheet and plate materials) is that the straight crack-front analysis generally over-predicts crack extension, before and after maximum load. A number of factors could be contributing to the discrepancies in crack extension, including crack-front tunneling, transition from initially flat fracture to slant fracture after maximum load, and the simplicity of the constant value of CTOA.

CTOA is a local fracture criterion that is always measured a fixed distance from the current crack tip. An alternative fracture criterion is δ_5, which is the displacement measured across the original crack tip location using a 5 mm gauge length. δ_5 is initially a local parameter, but after crack extension behaves more like a remote parameter. Figures 3 (a) and (b) show load-δ_5 plots for the 152 mm wide C(T) and 1016 mm wide M(T), respectively. In contrast to the load-crack extension comparisons, shown in Figure 2, the analysis matches the δ_5 behavior of the tests very well. The δ_5 results compared well before and after maximum load, corresponding respectively to the local and remote stages of crack extension. The results in Figure 3 (b) are somewhat abbreviated because the clip gage measuring δ_5 went out of range near the end of the test. However, data was collected past maximum load.

The results in Figure 3 strongly suggest that the flat, straight crack front in the 3D analysis represents the “average” crack length at any given load. Returning to Figure 2, the amount that the analysis over-predicts crack extension is on the order of the plate thickness. The crack extension was measured on the surface of the specimen during the test using a traveling-stage optical microscope. The surface measured value is the shortest crack length if the specimen is experiencing crack-front tunneling. A more appropriate comparison metric may be to use an average crack length measure, such as unloading compliance or an area average.

TUNNELING TESTS

Experiments and analyses were performed to characterize the crack tunneling for the 6.35 mm thick 2024-T351 aluminum alloy. The typical approach to characterize crack tunneling is to perform a multiple specimen test to obtain one crack-front per specimen [2]. In an effort to obtain more data per specimen, a combined approach was taken here. Three specimens are single crack-front tests, while the final specimen was used as a multiple crack-front specimen test.

A number of methods may be available to mark the crack fronts and measure the tunneling. Dye penetrants could be used while the crack is held open to take advantage of the capillary action at the crack. Radiographic measuring methodologies may be able to characterize the crack extension. Herein the crack front was marked with fatigue cycles at a high stress ratio (R = 0.75 or 0.8) and a relatively high load (80%

of the current fracture load). Typically about 2000 cycles were applied to mark the crack front. The crack front shapes were measured using an optical microscope with X-Y traveling stages.

Three C(T) specimens of width 152 mm were fatigue pre-crack at low stress levels (8 MPa $\sqrt{m}$) to an a/W of 0.4. Each specimen was loaded just enough to cause a predetermined amount of crack extension. Then the fracture crack front was marked using fatigue crack growth. For each specimen, some or all the of the following were collected: load, load-line displacement, crack-mouth-opening displacement, δ_5, unloading compliance, crack extension, and surface field displacements in the vicinity of the original crack tip. The amount of crack extension was based on the desire to characterize the tunneling progression along the crack front for various loading levels. The first specimen was loaded until about 0.25 mm of surface crack extension was visible. Two subsequent specimens were loaded to lower loads based on the unloading compliance load-crack extension curve. Table 1 summarizes the maximum load as well as maximum interior and surface crack extension values. The tunneling magnitude is $T = \Delta a_{max} - \Delta a_s$, where Δa_{max} is the crack extension on the interior, and Δa_s is the crack extension on the surface. The load corresponding to K_{Ic} for this material and configuration is about 10.7 KN.

Figure 4 shows the measured fatigue and fracture crack fronts from the multiple crack front specimen test. Also included in Figure 4 are the area-average (dash-dot) crack lengths for each crack front. Unloading compliance crack extension is somewhat less than area average and is omitted here for clarity. During the early stages of growth, for instance, at the lowest load from Table 1, the crack has some extension along nearly 80% of the fatigue crack-front. This extension was attained at only about 25% above the equivalent K_{Ic} load for this material, indicating that there may be relatively high constraint on the interior of the specimen encouraging growth at such low loads. The estimated plastic zone radius at this load is about 4 mm -- well beyond the limits of LEFM, but still smaller than the thickness. Additionally, this indicates that the crack extension may be retarded on the surface by plasticity, since surface-crack extension does not initiate until significant tunneling has taken place. Tunneling initially increases as the tensile fracture region develops, then as the shear lips form with increasing plasticity, tunneling decreases to an essentially constant value during fully developed slant fracture. The fatigue crack-front tunneling was about 12% of the plate thickness (B). Tunneling increases to about 40% of B when surface growth starts. After the flat-to-slant transition is complete, tunneling stabilizes at about 20% of B.

CRACK EXTENSION CALIBRATION

For tunneling cracks, there are, at least, four crack-length measurements: (1) crack length on the free surface, (2) unloading compliance crack length, (3) area-average crack length, and (4) maximum crack length in the interior. Figures 2 (a) and (b) compare experimentally measured surface values of crack extension with straight crack-front FEA results. Since tunneling does occur, it is desirable to account for the tunneling either in the analysis or in the test data. The most desirable approach is to modify the analysis to include crack-front shapes that match the experimental results [5] or use a modeling methodology that allows the tunneling to evolve naturally as part of the analysis [6]. However, these are cumbersome, time consuming, and not currently practical for industry. The alternative is to consider the experimental data and estimate crack extension using either unloading compliance or area average. Herein, the area-average values, based on the 9-point weighted average procedure [7], will be used, unless otherwise noted. Two situations exist requiring separate calibration curves: specimens that remain flat and specimens that exhibit the flat-to-slant crack transition. The process is essentially the same for the two fracture conditions using different calibration curves.

Figure 5 shows the tunneling magnitude, T, for the two fracture conditions. The tunneling for the flat-to-slant specimens was derived from Figure 4. The tunneling for the flat fracture is adapted from work by Dawicke et al. [5] for a thin sheet 2024-T3 aluminum alloy (scaled from B = 2.3 mm). Dawicke showed through experimental measurements similar to those from Figure 4 that for flat fracture, tunneling increased monotonically until it stabilized at a constant value. The curve for flat fracture in Figure 5 is a curve fit of Dawicke's data.

Figure 6 shows the area-average calibration curves derived from the flat and flat-to-slant crack data in Figure 5. The correction ratio, C_R, is the ratio of area average crack extension to the surface crack extension. The

curves are calculated using the equation for C_R in Figure 6 and the respective tunneling curves from Figure 5. The data points in Figure 6 are the calculated correction ratio based on the area average crack length from the measured tunneling. The f term in the C_R equation indicates what fraction of the tunneling magnitude represents the area average crack extension. For flat fracture the coefficient was determined from the area average crack length of Dawicke's [2] crack front shapes and is 0.64, and for slant fracture the coefficient was determined from the average of the tunneling data as 0.5.

Figure 7 compares data from Figure 2 corrected using the calibration curves for area-average crack extension with the analysis. Only data with $\Delta a > 0.2$ mm were corrected. As expected, both curves shifted significantly, resulting in a better match between the FEA and experimental results near maximum load. However, the analysis now significantly over-predicts the initiation load, indicating that a lower CTOA would be required in the analysis to predict initiation. From Table 1, crack initiation in the interior occurred before 13.3 KN, but the analysis did not initiate until about 19 KN. This is similar to the result by Dawicke et al. [5]. The crack-extension values for the flat specimen were larger than the value for the slant-crack specimens at a given load. Beyond maximum load, the measured surface crack-extension values were approximately the same in Figure 2 for the flat and slant specimens. The differences in the two curves in Figure 7 indicate that the importance of the failure mechanism (tensile versus shear) between the two failure modes may be more significant than was indicated by the surface measured crack-extension data of Figure 2.

CONCLUDING REMARKS

The excellent match between the experimental and analysis data in Figure 3 is compelling, and led us to consider the tunneling issue more carefully. The results in Figure 7 show better correlation between the corrected test data and the analysis results near maximum load, and showed that the constant CTOA fracture criterion transfers well between the fully constrained C(T) specimen and the wide, buckling M(T) specimens. The analysis was able to accurately predict the maximum load for C(T) specimens ranging in size from 50 mm to 152 mm and for M(T) specimens ranging in size from 75 mm to 1016 mm.

Optical measurement methods will likely remain the method of choice for the buckling wide panel tests. Unloading compliance measurements are difficult for buckling panels, and direct current potential difference (area average) can be somewhat difficult to set up and increases the complexity of the test procedure. However, unloading compliance is relatively straight-forward for constrained C(T) and M(T) specimens. If reliable tunneling test procedures can be developed, and if the material shows consistent tunneling behavior, then calibration procedures such as these presented here are viable.

REFERENCES

1. Harris, C.E., Newman, J. C., Jr., Piascik, R. and Starnes, J. H., Jr., "Analytical Methodology for Predicting the Onset of Widespread Fatigue Damage in Fuselage Structure," Journal of Aircraft, Vol. 35, No. 2, pp. 307-317, 1998.
2. Dawicke, D. S. and M. A. Sutton, "CTOA and Crack Tunneling Measurements in Thin Sheet 2024-T3 Aluminum Alloy," *Experimental Mechanics*, Volume 34 No. 4, pp. 357, 1994.
3. Wells, A.A., "Application of Fracture Mechanics at and Beyond General Yielding," *British Welding Journal*, Vol. 11, 1961, pp. 563-570.
4. James, M. A. and Newman, J. C., Jr., "Three Dimensional Analysis of Crack-Tip-Opening Angles and δ_5-Resistance Curves for 2024-T351 Aluminum Alloy," *Fatigue and Fracture Mechanics: 32nd Volume, ASTM STP 1406*, Ravinder Chona, Ed., American Society for Testing and Materials, West Conshohocken, PA, 2000 (in press).
5. Dawicke, D. S., J. C. Newman, Jr., and C. A. Bigelow, "Three-dimensional CTOA and Constraint Effects during Stable Tearing in Thin Sheet Material," *ASTM STP 1256*, W. G. Reuter, J. H. Underwood and J. C. Newman, Jr., Editors, American Society for Testing and Materials, pp. 223-242, 1995.
6. Ortiz, M. and Pandolfi, A., "Finite deformation irreversible cohesive elements for three-dimensional crack-propagation analysis," *Int J Num Meth Engng*, n 44, pp. 1267-1282, 1999.
7. ASTM Standard E1820, Volume 03.01, American Society for Testing and Materials, 2000.

TABLE 1
CRACK EXTENSION AT MAXIMUM APPLIED LOAD

Specimen	Load (KN)	Δa_s (mm)	Δa_{max} (mm)
1	24.4	0.25	2.0
2	17.8	0	0.6
3	13.3	0	0.1

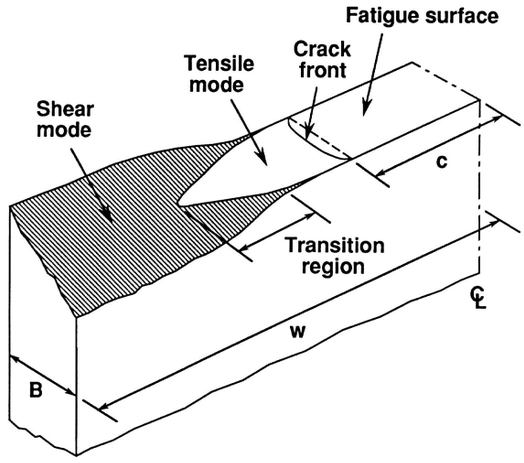

Figure 1: Schematic of a typical fracture surface

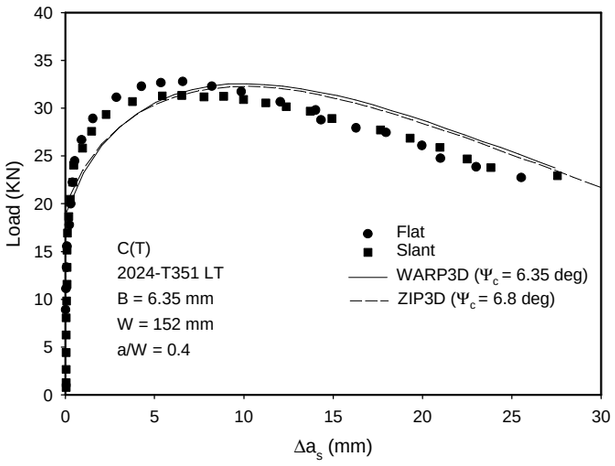

(a) 152 mm C(T)

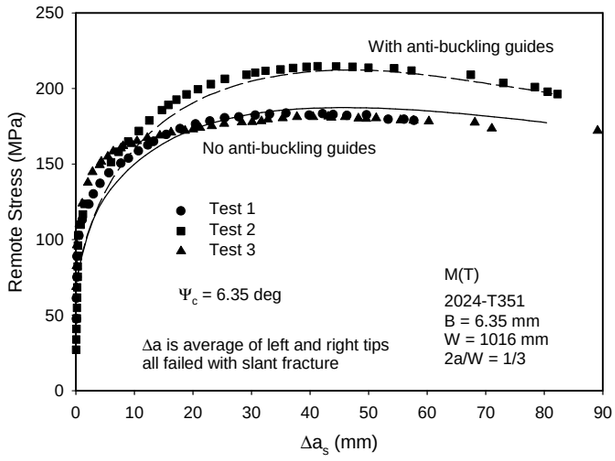

(b) 1016 mm M(T)

Figure 2: Experimental and numerical load-crack extension

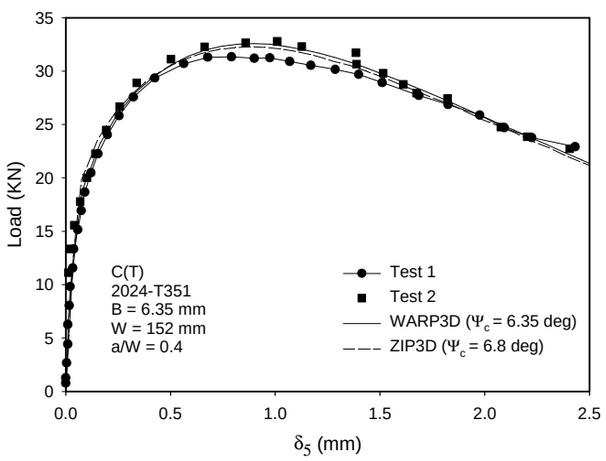

(a) 152 mm C(T)

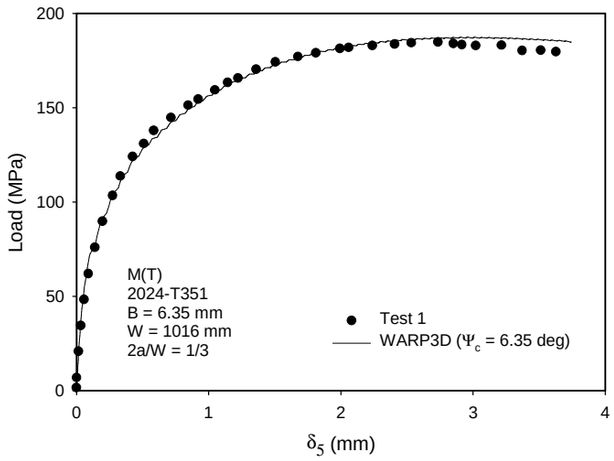

(b) 1016 mm M(T)

Figure 3: Experimental and numerical load- δ_5 results

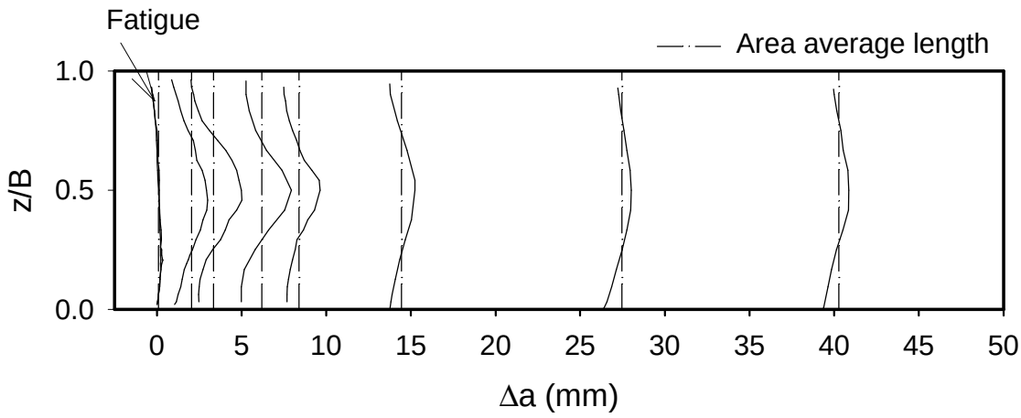

Figure 4: Optically measured fatigue and fracture crack-front shapes

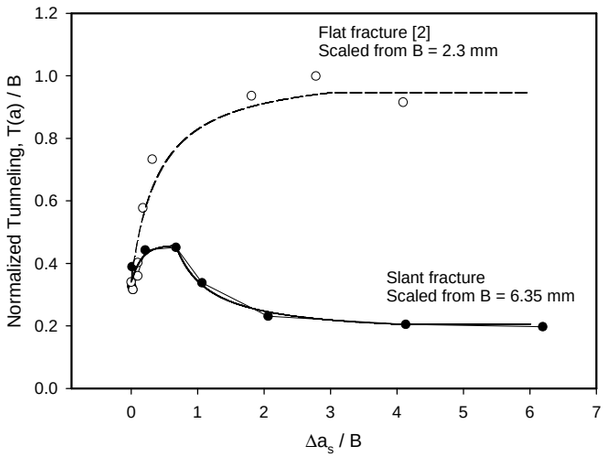

Figure 5: Tunneling magnitude for flat and flat-to-slant fracture surfaces

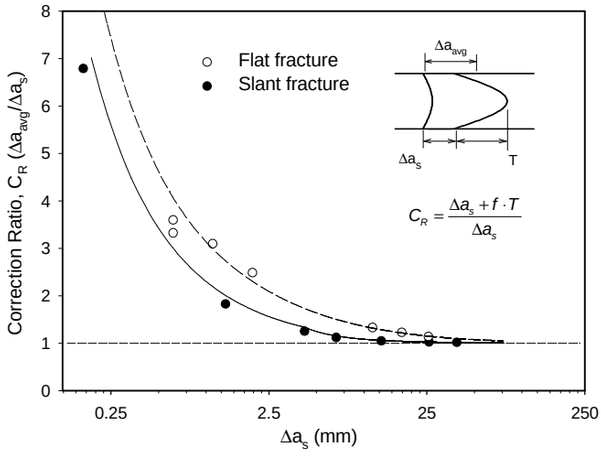

Figure 6: Area average calibration curves for flat and flat-to-slant fracture surfaces

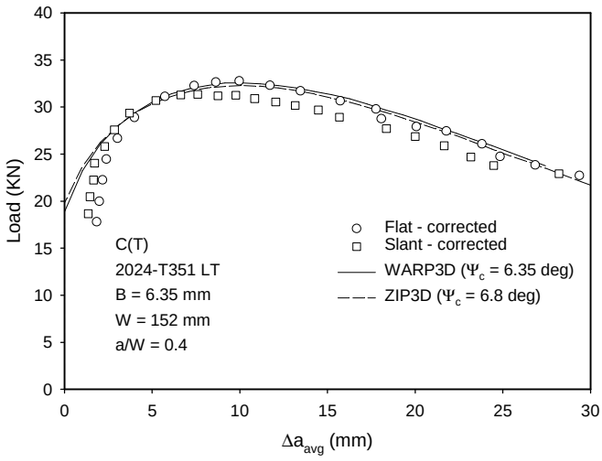

(a) 152 mm C(T)

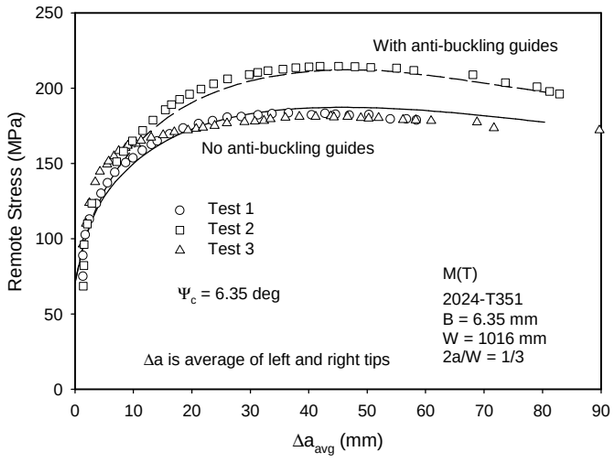

(b) 1016 mm M(T)

Figure 7: Corrected load-crack extension curves